NUEJ
Naresuan University
Engineering Journal

Maximum-Power-Point Tracking for Photovoltaic Arrays with Partial-Shading Detection

Peeradech Lousuwankun and Niphat Jantharamin*

Department of Electrical and Computer Engineering, Faculty of Engineering, Naresuan University, Phitsanulok, Thailand

*Corresponding author e-mail: niphatj@nu.ac.th

(Received: 14 December 2021, Revised: 18 February 2022, Accepted: 4 March 2022)

Abstract

In this paper, an approach to maximum-power-point tracking (MPPT) for photovoltaic (PV) arrays with partial-shading detection is demonstrated. The proposed MPPT algorithm consists of the incremental conductance (IncCond) technique with step-size variation, the partial-shading detection, and the scan for global maximum power point (GMPP) with search area restriction. The variable step size for MPPT relied on the change in array power and current. Inspection of irradiance condition was performed, so that the scan for GMPP over a voltage range occurred only if the partial shading was detected. Two partial-shading detection criteria were developed: the array was assumed to be partially shaded if just either of these two criteria was satisfied. Then, the array short-circuit current and open-circuit voltage under the present weather condition were also used for the search area restriction. After one side of the search area boundaries had been reached and the necessity of scan towards the other side was confirmed, the array operating point was then moved directly to its initial position to avoid retracing the route of search. Following the completion of scan, the array operating point was moved directly to the recorded GMPP without steady-state oscillation. In comparison to the two previously published algorithms, simulation results of the proposed MPPT technique indicated that the search area of GMPP could be narrowed by at least 20% under partial-shading conditions, and the tracking could be accelerated by about 90% under uniform irradiance.

Keywords: Maximum Power Point, Photovoltaic, Partial Shading, Incremental Conductance

1. INTRODUCTION

Solar energy has recently been a promising energy source for rural electrification. Direct conversion of solar energy into electricity is made possible by using a photovoltaic (PV) module. To increase the output electrical power, several PV modules are interconnected to form a PV array. However, the PV array power is strongly affected by weather variations. To maximize the PV array power related to each weather condition, the array operating point is placed at the maximum power point (MPP). This approach is called maximum-power-point tracking (MPPT), which can be achieved by regulating the PV array voltage, typically by means of a power converter. Partial shading, which can be caused by neighboring construction, trees, clouds or dirt on the array, results in uneven irradiance and has consequently negative effects on power-voltage characteristics of the array. According to the power-voltage curves in Fig. 1, a sole MPP exists under even irradiance condition. Apart from reduction in output power, the partial shading causes multiple peaks on the power-voltage curve. Among those peaks, the highest one is termed a global MPP (GMPP), and the others are called a local MPP (LMPP). The well-known MPPT methods, such as the perturb and observe (P&O) and the incremental conductance (IncCond), cannot effectively handle those multiple MPPs single-handed since their algorithms halt the tracking after a peak on the power-voltage characteristic curve, either a GMPP or an LMPP, is reached. If the operating point is stuck at the LMPP, the optimum power cannot be extracted from the array, which can be considered as a loss of array power. Therefore, an additional approach to track the GMPP is usually incorporated into the MPPT algorithm to obtain the optimum power output of the PV array under partial shading condition.

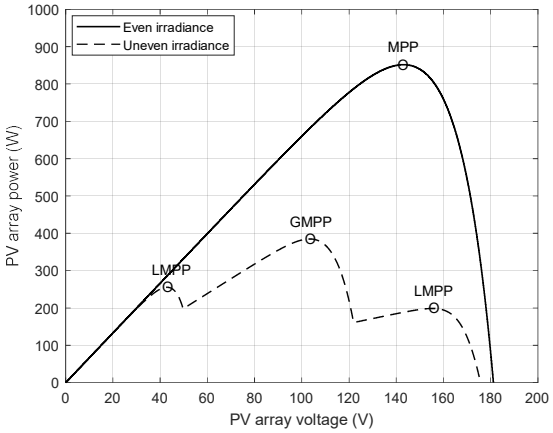

Figure 1 Effect of partial shading on a PV array power-voltage curve

Many GMPP tracking (GMPPT) techniques have been introduced in the literature. PV module rearrangement under each weather condition is presented by Elserougi et al. (2015), by which two certain configurations of modules are specified so that highest array power is investigated. Nonetheless, more strings of modules require more switches for the rearrangement, and tracking time is approximately doubled since two configurations are always implemented under each weather condition. As proposed by Ghasemi et al. (2018), speculation of the array current-voltage characteristics to specify the search area for the GMPP depends on the present operating point, the array open-circuit voltage under standard test conditions (STC: 1000 W/m^2, 25˚C) and the MPP of one module under the present weather condition. However, parameter determination for the speculation is complicated, and the operating point must be moved throughout the array voltage range. Based on the assumption that power at the peaks is increased or decreased consecutively, power observation at each peak of the array power-voltage curve contributes to knowledge of GMPP location without scanning the whole voltage range of the array (Tey & Mekhilef, 2014). The scheme is unfeasible for all partial-shading cases yet and causes the whole voltage-range search under uniform irradiance unnecessarily. Rough specification of the GMPP search area by using a linear mathematical equation derived from the short-circuit current and the open-circuit voltage of the array under present weather condition is presented by Ji et al. (2011). Consequently, the operating point is moved directly to a position assumed to be near the GMPP, and then moved towards the GMPP by means of the IncCond algorithm. Again, this approach is unfeasible for all partial-shading cases.

Furtado et al. (2018) and Ramana et al. (2019) present the P&O algorithm along with search area restriction for GMPPT, which is applicable to all characteristics of PV power-voltage curves under partial-shading conditions. The left boundary of the search area is specified by a minimum voltage which is derived from the ratio of the MPP current under STC. The right boundary used by Furtado et al. (2018) is fixed at 90% of the array open-circuit voltage under STC. On the other hand, the right boundary used by Ramana et al. (2019) is determined by a minimum current which is derived from the ratio of a newly discovered maximum power to 90% of the array open-circuit voltage under STC. During the scan for a GMPP, the search area becomes narrower if the power is found higher at each progressive step. In practice, however, the irradiance is typically lower than 1000 W/m^2 and when the solar cell temperature is higher than 25˚C, the search area is unnecessary wide. In addition, the scan is needlessly performed despite uniform irradiance since their algorithm lacks inspection of irradiance condition, and thus wastes tracking time. The linear relationship between the irradiance and the array short-circuit current can lead to partial-shading detection (Ahmed & Salam, 2017), which relies on the difference between irradiance values calculated from the module MPP current and from the array current at 80% of the array open-circuit voltage. However, numerous data collection is required for setting the criterion, and relocation of the operating point to the two aforesaid points for each irradiance condition inspection increases the tracking time.

Since the unnecessary scan under uniform irradiance caused by the GMPPT algorithms with search area restriction described above wastes the tracking time and can be considered as needless loss of the array output power, the partial shading detection technique can help the controller to avoid the dispensable scan and therefore reduce the array power losses. However, research on the incorporation of the partial shading algorithm into an MPPT approach has been very limited.

2. Proposed MPPT Method

The proposed MPPT technique incorporated the IncCond algorithm to avoid the steady-state oscillation of the array operating point. It included a new approach to detect the partial shading, and an improvement in search area restriction for GMPPT under partial shading situations. A search of GMPP usually takes much more time in comparison with a uniform irradiance case since a voltage scan up to the array open-circuit voltage is needed. Partial-shading detection can cause the GMPP scan to be used only if it is needed.

2.1 Partial-Shading Detection

Hereby, two partial-shading detection criteria were derived from the two approximately linear relationships, namely between the MPP current (I_{mpp}) and the short-circuit current (I_{sc}), and between the MPP voltage (V_{mpp}) and the open-circuit voltage (V_{oc}) of the PV array:

$$I_{mpp} \cong k_i \cdot I_{sc}\,, \tag{1}$$

$$V_{mpp} \cong k_v \cdot V_{oc}\,, \tag{2}$$

where k_i and k_v are constants. Typical current-voltage characteristic curves of a PV array under different incident irradiance conditions, on which small circles represent MPPs, are shown in Fig. 2. While the incident irradiance is uniform, only one MPP exists on the curve, as represented by the far-right curve. When the partial shading on the array happens, multiple MPPs appear on those curves, and the number of MPPs on each curve depends on shading patterns. On each curve of uneven irradiance cases, there is one MPP which gives the highest current produced by unshaded modules and this current value related to Eq. (1). Therefore, defined as the first detection criterion, the partial shading can be detected as soon as a measured MPP current is lower than the value obtained from Eq. (1).

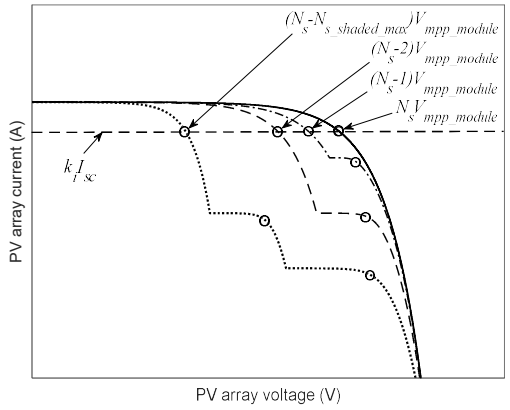

Figure 2 Current-voltage curves of a PV array under various partial shading conditions

In addition, the second detection criterion was based on the relationship between two conductance values of the array, namely the ratio of current to voltage at MPP (G_{mpp}) and the ratio of short-circuit current to open-circuit voltage (G_{ref}). Dividing Eq. (1) by Eq. (2) gives

$$\frac{I_{mpp}}{V_{mpp}} \cong \frac{k_i \cdot I_{sc}}{k_v \cdot V_{oc}}.$$

The above relationship can be written as

$$G_{mpp} \cong \frac{k_i}{k_v} \cdot G_{ref} \cong k_G \cdot G_{ref}. \quad (3)$$

where k_G is a constant and equals k_i/k_v. Equation (3) shows that G_{mpp} is directly proportional to G_{ref}. Moreover, the array MPP voltage under uniform irradiance is approximately equals the product of the module MPP voltage (V_{mpp_module}) and the module number in each string (N_s). As Fig. 2 shows, the MPP conductance of the unshaded array ($G_{mpp\_unshaded}$) can be obtained as

$$G_{mpp\_unshaded} = \frac{I_{mpp}}{N_s V_{mpp\_module}}. \quad (4)$$

According to Fig. 2, the array voltage at an MPP with highest current on each curve in partial shading cases approximately equals the product of the module MPP voltage and the difference between N_s and the maximum number of shaded modules in a string ($N_{s\_shaded\_max}$) compared with any other strings of the array. Therefore, the array conductance at this MPP (G_{mpp_shaded}) can be written as

$$G_{mpp\_shaded} = \frac{I_{mpp}}{(N_s - N_{s\_shaded\_max}) \cdot V_{mpp\_module}}.$$

Calculation of G_{mpp_shaded} can be formulated further as follows.

$$G_{mpp\_shaded} = \frac{I_{mpp}}{(N_s - N_{s\_shaded\_max}) \cdot V_{mpp\_module}} \times \frac{N_s}{N_s} = \frac{N_s}{(N_s - N_{s\_shaded\_max})} \times \frac{I_{mpp}}{N_s V_{mpp\_module}}.$$

Combining the above equation with Eq. (4) gives

$$G_{mpp\_shaded} = \frac{N_s}{(N_s - N_{s\_shaded\_max})} \times G_{mpp\_unshaded}. \quad (5)$$

Equation (5) shows that G_{mpp_shaded} is always higher than $G_{mpp\_unshaded}$ in each weather condition. As a result, the two partial-shading detection criteria can be summarized as follows.

First detection criterion: $I_{mpp} < k_{i\_min} \cdot I_{sc}$.

Second detection criterion: $G_{mpp} > k_G \cdot G_{ref}$.

If just either of these two criteria is satisfied, the array is assumed to be partially shaded. On the other hand, the incident irradiance is assumed to be equally distributed on the array if both criteria are untrue. In addition, the minimum value of k_i (k_{i_min}) is required in order that the first detection criterion is unmet in case of uniform irradiance. To determine k_{i_min} and k_G, details of MPP location were gathered from 450 PV module manufacturers in the database of MATLAB/Simulink. Current and voltage values of the MPPs under various weather conditions with evenly distributed irradiance are presented in Fig. 3, and their related k_i and k_v are shown in Fig. 4.

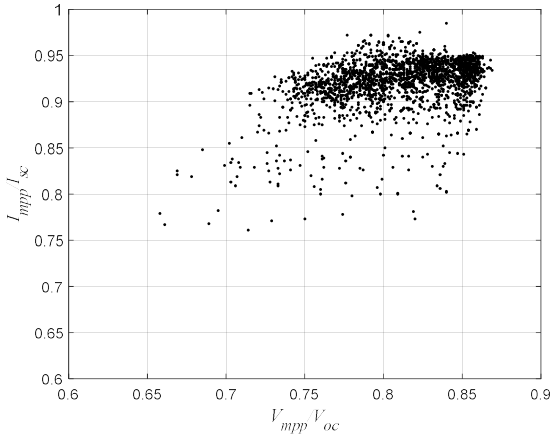

Figure 3 MPPs of 450 PV modules in various weather

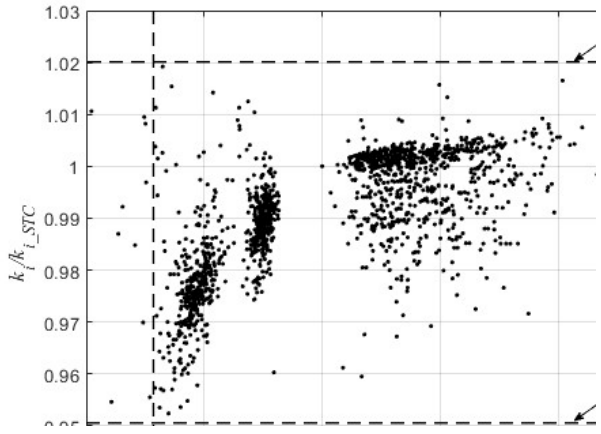

Figure 4 MPP current and voltage constants of 450 PV modules in various weather

Hence, k_{i_min} is specified to be 95% of k_i under STC (k_{i_STC}), and the minimum value of k_v (k_{v_min}) is selected to be 93% of k_v under STC (k_{v_STC}). Consequently, k_{i_min} and k_G for the partial-shading detection criteria are determined as follows.

$$k_{i\_min} = 0.95 k_{i\_STC}. \tag{6}$$

$$k_G = \frac{k_{i\_min}}{k_{v\_min}} = \frac{0.95 k_{i\_STC}}{0.93 k_{v\_STC}}. \tag{7}$$

2.2 Search Area Restriction

After the partial shading was detected, a search for GMPP location was initiated and the search area was limited. The search area restriction developed in this research was an improvement on the algorithm of Ramana et al. (2019). The ratio of newly discovered maximum power (P_{max}) to the product of k_i and the array short-circuit current under the present weather condition determined the minimum voltage (V_{min}), defined as the left boundary of the search area, under which P_{max} were never exceeded. Furthermore, the maximum value of k_i (k_{i_max}) was required in order that all MPPs existing under partial shading were included in the search area. According to Fig. 4, k_{i_max} was specified to be

$$k_{i\_max} = 1.02 k_{i\_STC}. \tag{8}$$

Thus, the left boundary of the search area was derived from

$$V_{min} = \frac{P_{max}}{k_{i\_max} I_{sc}}. \tag{9}$$

In addition, the right boundary of the search area was defined as the minimum current (I_{min}), which was derived from the ratio of P_{max} to 90% of the array open-circuit voltage under the present weather condition. Hence, the right boundary of the search area was calculated from

$$I_{min} = \frac{P_{max}}{0.9 V_{oc}}. \tag{10}$$

As the operating point was shifted during the scan for GMPPT and the array power higher than the latest P_{max} was detected, the values of P_{max}, V_{min} and I_{min} were updated and the voltage value at that point was recorded. The proposed concept of GMPPT within a search area can be described by using Fig. 5. As an example, the array was partially shaded, and the array operating point was currently at the point "P_A" while the system controller realized only the current and voltage values at the present operating point without knowledge of the power-voltage curve relative to the partial shading condition. Using Eqs. (9) and (10), the left boundary $V_{min,A}$ and the right boundary $I_{min,A}$ of the search area were determined. Hereby, the search algorithm started the scan by moving the operating point to the right, and hence higher power of the array was detected. According to Eqs. (9) and (10), the calculated values of V_{min} and I_{min} were higher, thus the left and right boundaries were updated. Accordingly, the search area became narrower until the point "P_B" was reached. Since the array power appeared lower on the right of P_B, the boundaries were unchanged. After the updated right boundary was reached and the scan continued in the opposite direction, the array power was still lower than P_B until the operating point was shifted through the point "P_D", beyond which the array power was higher than P_B, and the boundaries were then updated. The values of V_{min} and I_{min} were higher, and thus the search area became narrower until the point "P_E" was met. Since the array power appeared lower while moving the operating point to the left of P_E, the boundaries were unchanged, and hence the updated search area was determined by $V_{min,E}$ and $I_{min,E}$. The scan stopped after reaching the updated left boundary, and the GMPP location was consequently identified by the recorded voltage at which

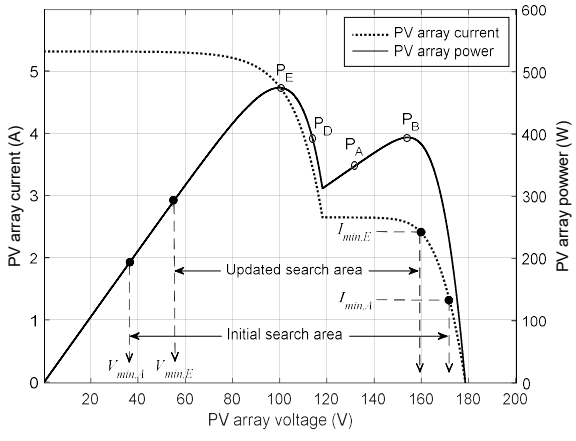

Figure 5 Search area restriction

P_{max} was given. The scan result was obtained identically even though the scan started with the operating point moved to the left first.

2.3 MPPT Algorithm

The proposed technique of MPPT started with a search for a closest MPP, then inspected the irradiance condition on the array, and finally performed GMPPT if the array was partially shaded, as described in Fig. 6. The values of k_{i_min} and k_G of the array were determined. The search for an MPP on the array power-voltage curve was based on the IncCond method with step-size variation presented by Lousuwankun & Jantharamin (2018), in which the determination of the desired step size depended on the change in array power and current, and can be expressed as

$$\Delta V_{pv}^{*} = \frac{\left|\Delta P_{pv}\right|}{V_{pv}\left|\frac{\Delta I_{pv}}{\Delta V_{pv,\max}}\right| + I_{pv}} \cdot \qquad (11)$$

ΔV_{pv}^{*} is the magnitude of desired array voltage variation and refers to the desired step size. ΔP_{pv} and ΔI_{pv} are the changes in array power and current respectively. $\Delta V_{pv,max}$ is the maximum magnitude of array voltage change, which is defined as the maximum step size.

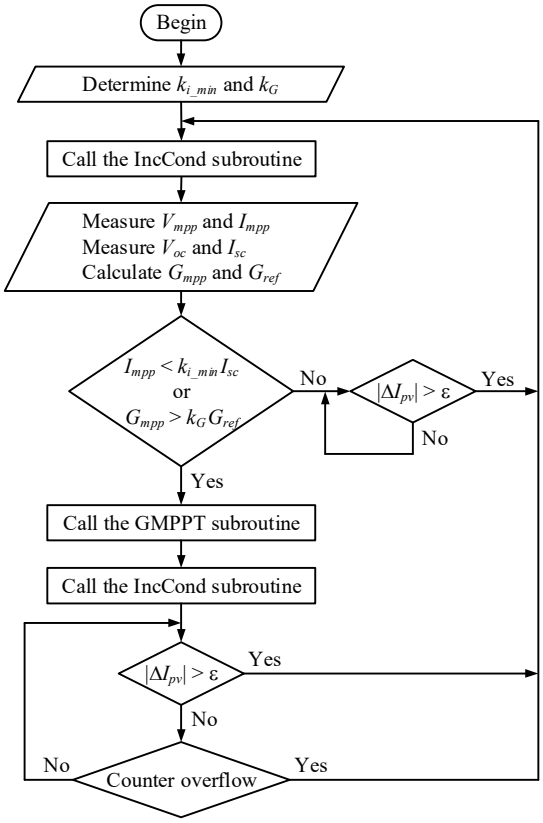

Figure 6 The proposed MPPT algorithm

After the first MPP was found, the irradiance condition on the array was examined. The voltage and current at this MPP, the open-circuit voltage and the short-circuit current of the array were measured. The two partial-shading detection criteria were inspected. If the incident solar intensity was uniform, the array operating point was kept at the present MPP until a change in array current was detected. On the other hand, if the partial shading on the array was detected, the GMPPT with the search area restriction was carried out. Then, the IncCond scheme was called again to locate the exact GMPP finely and the array operating point was kept there until a change in array current was noticed. However, the partial shading pattern on the array could change in such a way that the GMPP was shifted without a noticeable change in array current. Thus, a timer was set additionally after the GMPP was reached. Even if the array current fluctuation was undetected, the MPPT started over again after this certain amount of time elapsed to avoid the array operating point being separated from the GMPP for long.

The aforesaid GMPPT algorithm is described in Fig. 7. After the partial shading was detected, the scan for the GMPP started. The initial left- and right boundaries of the search area were determined by using Eqs. (9) and (10) respectively. Then, the array operating point was moved to the right and the array power value was observed. If the array power at each progressive step was higher than P_{max}, the array power and voltage values of that step were recorded. Hence, P_{max} and both sides of the search area were revised. After the updated right boundary was reached, the necessity of scan to the left boundary was examined. If the voltage at the updated left boundary was higher than the initial operating point voltage, the scan to the left boundary was needless. Thus, the scan was over, and the operating point was then moved to the GMPP related to the latest value of P_{max}. If the voltage at the updated left boundary was however lower than the starting-point voltage, the scan to the left boundary was still necessary. To avoid retracing the route of search, the operating point was moved to its initial position before the scan to the left was carried on. Again, if the array power at each progressive step was higher than P_{max}, the array power and voltage values of that step were recorded. P_{max} and both sides of the search area were therefore revised. Hence, the scan was complete after the updated left boundary was reached, and the operating point was then moved to the GMPP related to the latest value of P_{max}.

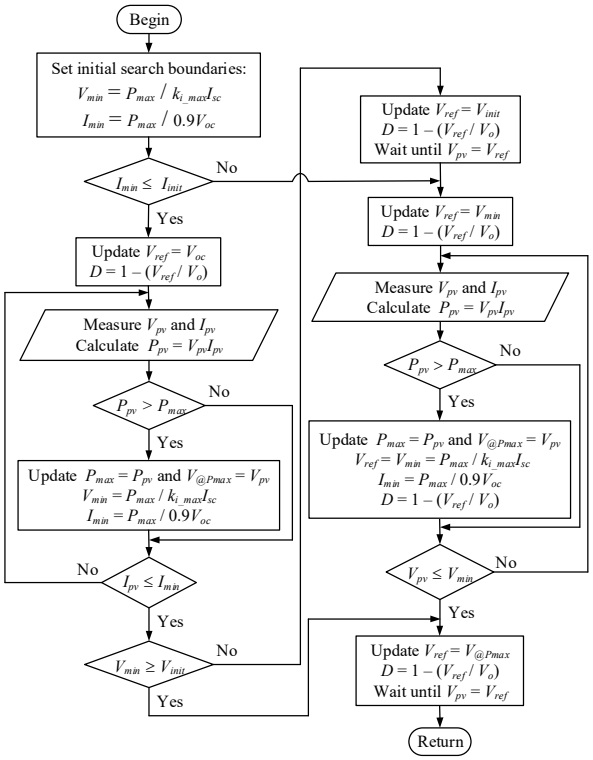

Figure 7 GMPPT algorithm of the proposed technique

2.4 PV System Using a Boost Converter for MPPT

PV array power maximization is typically realized by means of a power converter. A DC boost converter was hereby selected for tracking the MPP, and hence located between the array and a battery bank which served as load of the system as indicated in Fig. 8. The switches S_1 and S_2 contributed to momentary measurement of the array open-circuit voltage and short-circuit current. In a system normal operation, S_1 was open and S_2 was close, the capacitor C_1 was consequently situated over the array terminal, and thus its voltage dictated the array voltage. The performance of the boost converter depended upon switching. The switch duty cycle influenced the voltage of the capacitor C_1 and hence the PV voltage. The characteristic of battery bank was described by a series connection model of a resistor R_b representing the battery internal losses and a capacitor C_b explaining the battery bank capacity. As required, S_1 was first turned off, and thus the voltage en open-circuit voltage value to the controller, S_2 was then turned on, so the current sensor gave the array short-circuit current value to the controller while C_1 acted as a sole voltage source of the circuit. After the temporary measurement, S_2 was turned off and then S_1 was turned on, so C_1 was connected across the array terminal again.

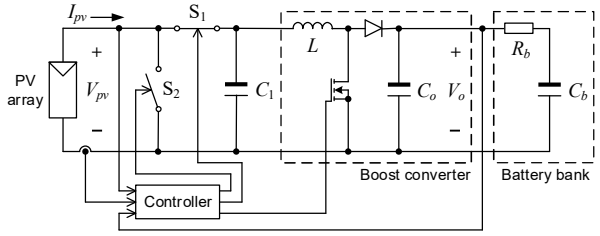

Figure 8 PV system circuit diagram for MPPT

Regarding Fig. 8, chosen parameters of the boost converter and the battery bank were as follows: C_1 = 4700 μF, L = 1 mH, C_o = 1000 μF, switching frequency = 20 kHz; R_b = 0.5 Ω, and C_b = 47 F. In this simulation, the PV array consisted of 2 parallel strings of modules, each of which was formed from 10 modules connected in series. Under STC, the array produced the short-circuit current of 6.66 A, the open-circuit voltage of 181 V and the maximum power of 851 W at 143 V. The array also gives k_{i_STC} of 0.89 and k_{v_STC} of 0.79. Thus,

$$k_{i\_min} = 0.95 k_{i\_STC} = 0.95 \times 0.89 = 0.84,$$

$$k_{i\_max} = 1.02 k_{i\_STC} = 1.02 \times 0.89 = 0.91,$$

and $$k_G = \frac{0.95 k_{i\_STC}}{0.93 k_{v\_STC}} = \frac{0.95 \times 0.89}{0.93 \times 0.79} = 1.15 .$$

3. SIMULATION RESULTS

The PV array was exposed to three environmental conditions consecutively, namely two partial shading conditions and one uniform irradiance situation respectively, as shown in Fig. 9. Under the first condition, the solar cell temperature was 25˚C, six modules of the array were exposed to 500 W/m^2, eight modules were partially shaded to 400 W/m^2, and six modules were incompletely shaded to 200 W/m^2. Then, the array experienced the second condition, under which four modules were exposed to 500 W/m^2, and sixteen modules were partially shaded to 400 W/m^2 while the solar cell temperature remained 25˚C. Finally, the third condition referred to the situation in which the equally distributed irradiance of 400 W/m^2 was incident on the array and the solar cell temperature rose to 27˚C. The array power-voltage characteristic curves related to each irradiance condition are indicated in Fig. 10. Even though higher cell temperature causes the array power to drop and the location of MPPs on the array power-voltage curve to be shifted to the left, a change in the cell temperature has no influence on the tracking performance of the purposed algorithm. Therefore, the cell temperature effect was not emphasized in this simulation.

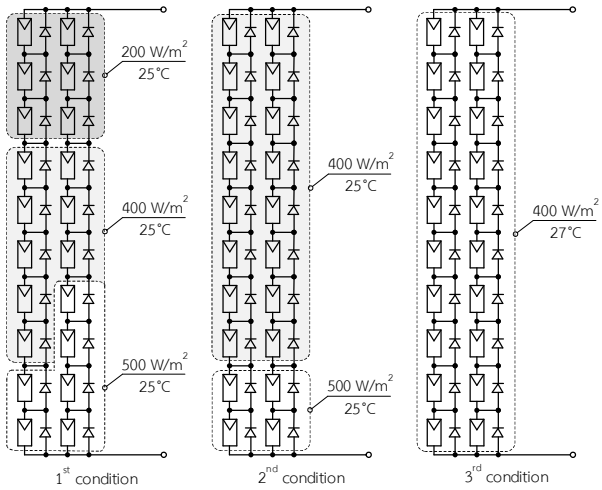

Figure 9 Irradiance conditions on the PV array

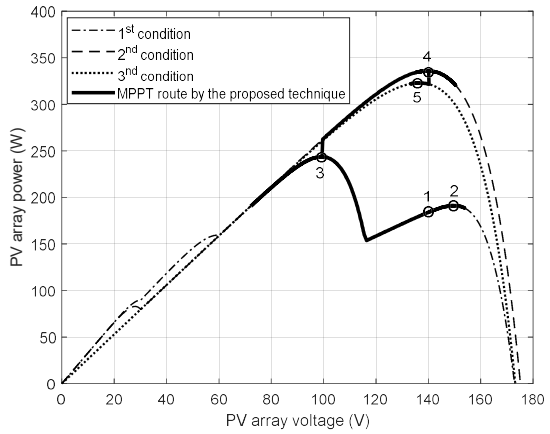

Figure 10 Operating point movement during MPPT

Regarding the width of search area and the true-MPP tracking time, the simulation results of the proposed technique were compared with those obtained from the algorithms previously published by Furtado et al. (2018) and Ramana et al. (2019). The traditional P&O algorithm was also implemented in the simulation for the MPPT performance comparison. The PV array voltage variation during the MPPT is shown in Fig. 11, and the related PV array power fluctuation is illustrated in Fig. 12. At first, the array experienced the first weather condition, under which a partial shading happened as described in Fig. 9. The initial duty cycle of the boost converter caused the operating point to be at 'Point 1' in Fig. 10. The MPPT was commenced after 0.1 s elapsed. The P&O algorithm caused the operating point to be stuck at the LMPP at 'Point 2', at which the array delivered 191.2 W, and thus failed to track the GMPP, at which the array could give 243.5 W. Hence, the P&O algorithm resulted in 21.5% loss of array power. However, the proposed technique and the other two algorithms were able to move the operating point to the GMPP at 'Point 3' eventually. According to the graphs in Fig. 11, the algorithms of Furtado et al. (2018) and Ramana et al. (2019) provided the search area of 121 V and 102 V, or 70% and 59% of the present array open-circuit voltage (173.2 V), with the tracking time of 0.37 s and 0.22 s respectively. However, the proposed technique gave the search area of 81.7 V, or 47.2% of the present array open-circuit voltage, with the tracking time of 0.26 s. In comparison with the algorithms of Furtado et al. (2018) and Ramana et al. (2019), the proposed technique contributed therefore to the search area narrowed by 32.5% and 20% respectively, with 29.7% higher tracking speed compared with the algorithm of Furtado et al. (2018) and 18.2% longer tracking time compared to the algorithm of Ramana et al. (2019).

After 0.8 s passed, the array encountered another partial shading condition as specified to the second weather condition. The operating point was then moved to the present GMPP at 'Point 4'. the algorithms of Furtado et al. (2018) and Ramana et al. (2019) gave the search area of 104 V and 109.5 V, or 59.4% and 62.5% of the present array open-circuit voltage (175.2 V), with the tracking time of 0.41 s and 0.3 s respectively. Nonetheless, the proposed method gave the search area of 50.8 V, or 29% of the present array open-circuit voltage, with the tracking time of 0.2 s. In comparison with the algorithms of Furtado et al. (2018) and Ramana et al. (2019), the proposed method contributed therefore to the search area narrowed by 51.1% and 53.6%, and thus the tracking speed increased by 50% and 32.3% respectively. On the other hand, the P&O technique resulted in the fastest tracking time of 70 ms since the LMPP voltage under the previous weather condition (at 'Point 2') was closest to the present GMPP voltage (at 'Point 4').

After 1.3 s elapsed, the array was exposed to the third weather condition, under which the incident solar radiation was uniform. The operating point was then moved to the present MPP at 'Point 5'. The algorithms of Furtado et al. (2018) and Ramana et al. (2019) provided the search area of 106 V and 98.5 V, or 61.1% and 57% of the present array open-circuit voltage (173.2 V), with the tracking time of 0.33 s and 0.3 s respectively. On the other hand, the proposed approach performed the MPPT without scanning voltage over a search area since no partial shading occurred, and results in the tracking time of 32 ms. While the P&O method spent 62 ms to reach the present MPP, the proposed technique provided faster tracking speed by 48.4%. In comparison with the algorithms of Furtado et al. (2018) and Ramana et al. (2019), the proposed approach contributed therefore to the tracking speed increased by 90.3% and 89.3% respectively. As a result, the operating point movement towards the true MPP related to each irradiance condition, which was caused by the proposed technique, is indicated in Fig. 10.

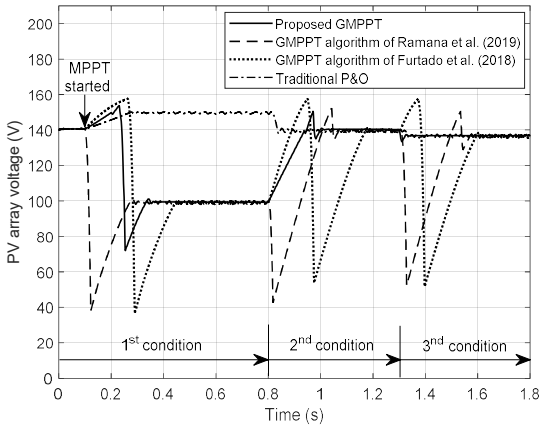

Figure 11 PV array voltage variation during MPPT

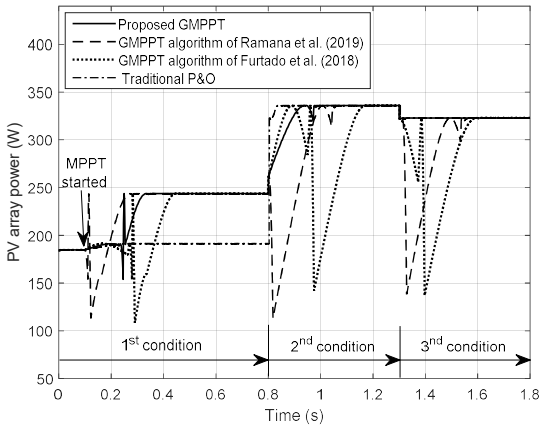

Figure 12 PV array power fluctuation during MPPT

4. DISCUSSIONS

By means of simulation, the width of search area and the speed of MPPT, which resulted from the proposed technique, were compared with those obtained from the algorithms of Furtado et al. (2018) and Ramana et al. (2019). The search area restriction of the proposed MPPT technique was based on the short-circuit current, the open-circuit voltage, and the newly discovered output power of the array under the present weather condition. However, the search area restriction by the algorithms of Furtado et al. (2018) and Ramana et al. (2019) were based on the MPP current and the open-circuit voltage of the array under STC (1000 W/m^2, 25˚C). In addition, the right boundary of the search area created by the algorithm of Furtado et al. (2018) was fixed. Since the simulated irradiance level was lower than 1000 W/m^2, the short-circuit current value used by the proposed technique was lower and therefore resulted in a narrower search area.

The tracking time, which can refer to the tracking speed, is affected by the scan procedure for a GMPP. Regarding the algorithms of Furtado et al. (2018) and Ramana et al. (2019), the operating point was slid to meet one boundary of the search area, and then moved in reverse until it hit the opposite boundary. Hence, backtracking occurred during each scan, and reduced the tracking speed. The proposed technique, however, examined the necessity of scan in reverse after the operating point had met the right boundary. If the scan to the left boundary was needed, the operating point was moved directly to its initial position to avoid going back the same route as demonstrated in case of the first weather condition. If the scan in reverse was unnecessary as shown in case of the second weather condition, the scan was finished, and thus the tracking time was saved. In addition, the traditional P&O algorithm could easily fail to track the GMPP under partial-shading conditions if a LMPP was found first, resulting in loss of array power.

Following the scan throughout the search area, the proposed technique resulted in the operating point being moved directly to the recorded GMPP without a steady-state oscillation due to the IncCond approach with step-size adaptation. The algorithms of Furtado et al. (2018) and Ramana et al. (2019), on the other hand, caused the operating point to oscillate around the MPP due to the P&O scheme. Moreover, they performed the scan even though the incident solar intensity on the array was uniform as presented in case of the third weather condition, thus lost power during the scan and wasted tracking time since a sole MPP was present. The proposed technique, however, searched for the closest MPP and inspected the irradiance condition on the array. Since no partial shading was detected, the operating point was kept at that MPP without performing the unnecessary scan. Based on the step-size variation, the proposed technique was superior to the traditional P&O algorithm in terms of MPP tracking speed.

5. CONCLUSIONS

This paper presented the MPPT approach under partial-shading condition, which was made up of the IncCond technique with step-size variation, the partial-shading detection, and the scan for GMPP with search area restriction. Irradiance condition on the array was investigated, so that the GMPP search over a voltage range is carried out only if the partial shading was detected. Partial-shading detection was based on two criteria, which were analytically devised by using details of MPP location collected from 450 PV module manufacturers in MATLAB/Simulink database. The first criterion involved the MPP current and the short-circuit current. The second criterion relied on the output conductance at the MPP, and the reference conductance derived from the ratio of short-circuit current to open-circuit voltage under the present weather condition. If just either of these two criteria was fulfilled, the irradiance on the array was assumed to be uneven. Then, the array short-circuit current and open-circuit voltage under the present weather condition were also applied for the search area restriction. After the right boundary

of the search area had been met and the scan to the left boundary was obliged, the array operating point was then moved straight to its original location to avert going back the same route before the scan was continued to the left. Compared with the algorithms of Furtado et al. (2018) and Ramana et al. (2019), simulation results under partial-shading conditions showed that the proposed MPPT approach provided a narrower area of GMPP search and higher tracking speed. In case of a uniform irradiance, the proposed technique performed no scan over a search area and therefore saved the tracking time substantially. Future work on this research will focus on validation of the proposed technique, which includes development of an embedded controller and a hardware prototype.

6. ACKNOWLEDGMENT

The authors are grateful to the Faculty of Engineering, Naresuan University for supporting this research financially and also providing research facilities.

7. REFERENCES

Ahmed, J. & Salam, Z. (2017). An Accurate Method for MPPT to Detect the Partial Shading Occurrence in a PV System. *IEEE Transactions on Industrial Informatics*, *13*(5), 2151–2160. https://doi.org/10.1109/TII.2017.2703079

Elserougi, A. A., Diab, M. S., Massoud, A. M., Abdel-Khalik, A. S. & Ahmed, S. (2015). A Switched PV Approach for Extracted Maximum Power Enhancement of PV Arrays During Partial Shading. *IEEE Transactions on Sustainable Energy*, *6*(3), 767–772. https://doi.org/10.1109/APEC.2015.7104786

Furtado, A. M. S., Bradaschia, F., Cavalcanti, M. C. & Limongi, L. R. (2018). A Reduced Voltage Range Global Maximum-power-point tracking Algorithm for Photovoltaic Systems Under Partial Shading Conditions. *IEEE Transactions on Industrial Electronics*, *65*(4), 3252–3262. https://doi.org/10.1109/TIE.2017.2750623

Ghasemi, M. A., Ramyar, A. & Iman-Eini, H. (2018). MPPT Method for PV Systems Under Partially Shaded Conditions by Approximating *I–V* Curve. *IEEE Transactions on Industrial Electronics*, *65*(5), 3966–3975. https://doi.org/10.1109/TIE.2017.2764840

Ji, Y.-H.; Jung, D.-Y.; Kim, J.-G.; Kim, J.-H.; Lee, T.-W.; Won, C.-Y. (2011). A Real Maximum-power-point tracking Method for Mismatching Compensation in PV Array Under Partially Shaded Conditions. *IEEE Transactions on Power Electronics*, *26*(4), 1001–1009. https://doi.org/10.1109/TPEL.2010.2089537

Lousuwankun, P. & Jantharamin, N. (2018). Photovoltaic Module Maximum-Power-Point Tracking with Step-Size Variation. *2018 International Conference on Engineering, Applied Sciences, and Technology*, pp. 1-4, https://doi.org/10.1109/ ICEAST.2018.8434450

Ramana, V. V., Mudlapur, A., Damodaran, R. V., Venkatesaperumal, B. & Mishra, S. (2019). Global Peak Tracking of Photovoltaic Array Under Mismatching Conditions Using Current Control. *IEEE Transactions on Energy Conversion*, *34*(1), 313–320. https://doi.org/10.1109/TEC.2018.2873667

Tey, K. S. & Mekhilef, S. (2014). Modified Incremental Conductance Algorithm for Photovoltaic System Under Partial Shading Conditions and Load Variation. IEEE Transactions on Industrial Electronics, 61(10), 5384–5392. https:// doi.org/10.1109/TIE.2014.2304921

8. BIOGRAPHIES

Peeradech Lousuwankul received the B.Eng. and M.Eng. from Naresuan University in 2017 and 2019 respectively. All degrees are in Electrical Engineering. He studies now towards a research Ph.D. degree in Electrical Engineering at the Faculty of Engineering, Naresuan University in Phitsanulok province, Thailand.

Dr. Niphat Jantharamin received the B.Eng. from King Mongkut's Institute of Technology Ladkrabang (KMITL), Thailand in 1997, the M.Sc. from the University of Kassel, Germany in 2002 and the Ph.D. from the University of Leeds, UK in 2008. All degrees are in Electrical Engineering. He is currently an Associate Professor of Electrical Engineering at Naresuan University, in Phitsanulok province, Thailand. His research interests include Power Electronics, Photovoltaic system technology and efficient energy conversion.